# Comparison of Iodine-123-Iomazenil SPECT and Technetium-99m-HMPAO-SPECT in Alzheimer's Disease

Kazuki Fukuchi, Kazuo Hashikawa, Yujiro Seike, Hiroshi Moriwaki, Naohiko Oku, Mariko Ishida, Masahiro Fujita, Toshiisa Uehara, Hirotaka Tanabe, Hideo Kusuoka and Tsunehiko Nishimura

*Division of Tracer Kinetics, Biomedical Research Center, First Department of Internal Medicine and Third Division of Medical Science for Health, Faculty of Health and Sports Science, Osaka University Medical School, Suita, Osaka, Japan*

This study was designed to elucidate a central type of benzodiazepine (Bz) receptor distribution in patients with Alzheimer's disease using SPECT with [$^{123}$I]iomazenil (IMZ). **Methods:** Eight patients with probable Alzheimer's disease were studied. Benzodiazepine receptor imaging was performed 15 min (early) and 180 min (delayed) after intravenous administration of 167 MBq IMZ, sequentially, using hexamethylpropylene amine oxime (HMPAO) SPECT to evaluate regional cerebral perfusion. **Results:** Early IMZ-SPECT depicted areas of reduced uptake in sites of decreased cerebral blood flow (CBF), but each area of decreased uptake was extended wider than the area of hypoperfusion. Delayed IMZ-SPECT images demonstrated a similar pattern of decreased area of CBF; the affected region in Bz receptor bindings, however, was clearer and broader compared with that in either HMPAO-SPECT or early IMZ-SPECT. In comparison with the uptakes for the normal cerebral hemisphere (ratio to the contralateral cerebellum) in patients with unilateral cerebral infarction as a control group ($n = 4$), the patients with Alzheimer's disease showed distinctive bilateral frontal or parietal defects ($p < 0.05$). **Conclusion:** Brain SPECT using IMZ may be more sensitive than CBF images in patients with Alzheimer's disease.

**Key Words:** benzodiazepine receptor; Alzheimer's disease; iodine-123-iomazenil; technetium-99m-HMPAO

**J Nucl Med 1997; 38:467–470**

Brain perfusion SPECT is useful in the diagnostic evaluation of patients with memory and cognitive abnormalities. In Alzheimer's disease, especially, the predominant finding of bilateral posterior temporal and parietal perfusion defects in these patients is highly predictive of the disease (*1*). Otherwise, previous studies have revealed reduction of several neurochemical markers in Alzheimer's disease in postmortem observation (*2,3*). As a neuroreceptor imaging modality, SPECT has played a very limited role in clinical practice. However, in the last few years, SPECT ligands have been developed for several neuroreceptor imaging techniques. After the synthesis of $^{123}$I-Ro 16-0154 (iomazenil), a flumazenil analog labeled with $^{123}$I, some trials have shown that this ligand visualizes the gamma-aminobutyric acid/benzodiazepine (Bz) receptor complex in healthy volunteers and in patients with neurologic disorders (*4–6*). Postmortem observation revealed that Bz receptor binding sites were significantly reduced in the frontal cortex, the temporal cortex and the hippocampus in Alzheimer's disease (*7*).

To determine the potential utility of [$^{123}$I]iomazenil (IMZ) SPECT in the evaluation of Alzheimer's disease, we compared the distributions of IMZ and the flow tracer, $^{99m}$Tc-hexamethylpropylene amine oxime (HMPAO), in patients diagnosed with probable Alzheimer's disease in the moderate stage based on the clinical symptoms.

Received Mar. 4, 1996; revision accepted Jul.1, 1996.

For correspondence or reprints contact: Tsunehiko Nishimura, MD, PhD, Division of Tracer Kinetics, Biomedical Research Center, Osaka University Medical School, Yamada-oka 2-2, Suita, Osaka 565, Japan.

## METHODS

### Subjects

Eight patients (4 men, 4 women; mean age 57.5 yr; range 55–61 yr) underwent IMZ and HMPAO-SPECT. The patients' clinical manifestations fulfilled the criteria for probable Alzheimer's disease proposed by NINCDS-ADRDA (*8*). All patients had a history of gradually progressive intellectual deterioration without focal motor or sensory signs and a laboratory examination profile that was negative for other major illnesses. The MRI and/or CT findings were negative except for signs of mild generalized atrophy. To evaluate the clinical symptoms of the subjects, a single experienced neuropsychologist (H.T.) performed neurological and neuropsychological examinations. The Mini-Mental State Examination and Raven's Colored Progressive Matrices were also administered to assess the clinical symptoms. The clinical features of the subjects are summarized in Table 1. For the control group, four patients with unilateral cerebral infarction (4 men, mean age, 51.3 yr) were adopted. There were no abnormalities according to MRI or brain perfusion SPECT images in their unaffected cerebral hemispheres.

Informed consent, using guidelines established by Osaka University Medical School, was obtained from the patients or their next of kin.

### Scan Acquisition and Image Processing

The subjects were studied in the awake-resting state and were not sedated before tracer injection or during the course of the examination to prevent any effect of the sedative on cerebral perfusion or Bz receptor bindings. For brain perfusion SPECT, $^{99m}$Tc-HMPAO was prepared according to the manufacturer's recommendations, and a 740-MBq dose was administered by intravenous bolus injection. Image acquisition began after approximately 5 min. IMZ-SPECT imaging was performed at 15 min (early images) and 180 min (delayed images) postadministration of 167 MBq IMZ. In each patient, the HMPAO- and IMZ-SPECT examinations were performed at a mean interval of 1.36 mo. During both studies, no changes in clinical features were found in any of the patients. Both SPECT scans were acquired using a high-performance, four-head rotating gamma camera equipped with low-energy, general-purpose collimators (*9*). SPECT acquisition was performed in 64 steps, 360° and with a $64 \times 64$ matrix ($4 \times 4$ mm per pixel). SPECT acquisition datasets were prefiltered with a Butterworth filter, then reconstructed with a Ramachandran

**TABLE 1**
Clinical Data for Alzheimer's Disease Patients

| Patient no. | Age (yr) | Sex | Neurological dysfunctions | | | | | | MMSE (/30) | RCPM (/36) |
|---|---|---|---|---|---|---|---|---|---|---|
| | | | MD | VSD | WFD | AC | LOI | PC | | |
| 1 | 57 | M | + | + | − | + | − | − | 25 | 18 |
| 2 | 55 | F | + | + | − | − | + | − | 21 | 20 |
| 3 | 57 | F | + | + | + | + | + | − | 11 | 13 |
| 4 | 57 | M | + | + | + | na | + | − | 16 | 13 |
| 5 | 56 | M | + | + | + | + | + | − | 23 | 23 |
| 6 | 56 | F | + | + | + | + | + | + | 23 | 24 |
| 7 | 61 | M | + | + | + | − | + | + | 20 | 17 |
| 8 | 61 | F | + | + | − | + | + | ± | 24 | 31 |

MD = memory disturbance; VSD = visuospatial disturbance; WFD = word-finding difficulty; AC = acalculia; LOI = lack of insight; PC = personality change; MMSE = Mini-Mental State Examination; RCPM = Raven's Colored Progressive Matrices; na = not available.

backprojection filter. Chang's postreconstruction attenuation correction was applied with an attenuation coefficient of 0.08 $cm^{-1}$ to the transaxial image data. The final reconstructed transaxial image was generated from 8-mm-thick slices. The transaxial spatial resolution was 13.0 mm in FWHM.

### Image Analysis

For qualitative visual interpretation of tomographic images, all transaxial slices were displayed on the computer screen as well as on recorded hard copy film. All tomographic images were interpreted blindly (without knowledge of clinical history) by three nuclear medicine physicians (K.F., K.H. and Y.S.) who evaluated sets of early and delayed IMZ-SPECT and HMPAO-SPECT from the same patients independently. Observers judged image sets for the composite defect sizes of early IMZ, delayed IMZ and HMPAO for each patient, individually. For this interpretation, the observers consulted the normal distribution of IMZ as published in previous reports (*10,11*). The interobserver agreement rate for the three observers was 92% (22/24; total for early IMZ, delayed IMZ and HMPAO) for the SPECT images.

### Evaluation of Bz Receptor Imaging of Iodine-123-IMZ

Semiquantitative analysis of delayed IMZ-SPECT was performed using the region of interest (ROI) method. ROIs were outlined manually in three representative SPECT images corresponding to the level of the centrum semiovale, basal ganglia and cerebellum on the frontal cortex, parietal cortex, temporal cortex, occipital cortex and cerebellum as previously described (*12,13*). In patients with Alzheimer's disease, the average counts per pixel of each cortical area were then divided by the average counts per pixel found in the cerebellar hemisphere with the highest activity. In patients with unilateral cerebral infarction, the average counts of the unaffected cerebral hemisphere were divided by those of the contralateral cerebellum. These ratios for patients with Alzheimer's disease were compared with the ones obtained for cerebral infarction patients.

### Statistical Analysis

Data are expressed as the mean ± s.d. The Student's t-test for nonpaired samples was used to compare the results obtained for each of these groups. A probability level of less than 0.05 was considered to indicate a significant difference.

## RESULTS

### HMPAO-SPECT Versus IMZ-SPECT

HMPAO-SPECT and IMZ-SPECT findings are summarized in Table 2. In HMPAO-SPECT scans, all of the patients showed perfusion abnormalities. The decreased flow depicted on the images was classified into one of the three patterns of temporo-parieto-occipital (TPO) hypoperfusion, frontal predominant (F) hypoperfusion and hypoperfusion in both areas (F+TPO). In four patients (Patients 1–4), HMPAO-SPECT demonstrated hypoperfusion in bilateral TPO regions. In those patients, early and delayed IMZ-SPECT showed reduced uptake areas more clearly and more extensively than HMPAO-SPECT. In the comparison between early and delayed IMZ-SPECT, delayed IMZ-SPECT images showed decreased uptake over a wider area than did HMPAO-SPECT (Fig. 1). In Patients 2 and 4, whose brain perfusion abnormalities were mild and localized within a small region, the area of decreased uptake of IMZ-SPECT extended into the superior parietal areas. In three patients (Patients 6–8) with F hypoperfusion, early IMZ-SPECT findings showed areas of decreased uptake located in the bilateral frontal lobes, and these were wider than those depicted by HMPAO-SPECT (Fig. 2). In Patient 5, who had bilateral F+TPO hypoperfusion, the abnormalities seen on both early and delayed IMZ-SPECT images showed similar patterns to those seen on perfusion images. However, the affected areas

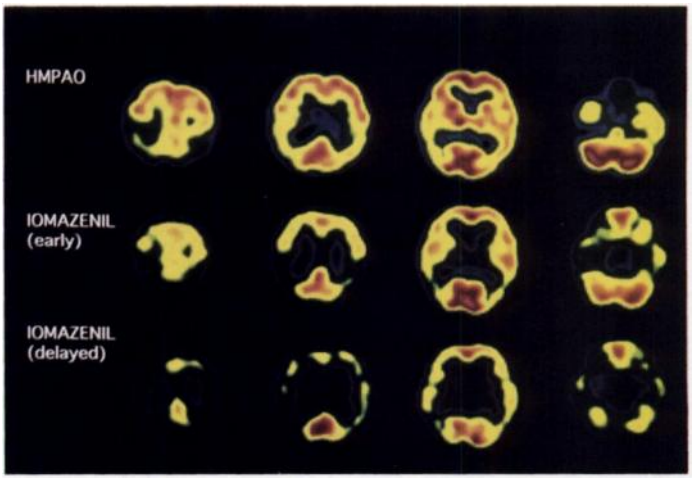


**FIGURE 1.** Patient 2, a 55-yr-old woman with Alzheimer's disease. HMPAO-SPECT (top) shows reduced uptake in bilateral TPO regions with no other sites of reduced uptake. Early IMZ-SPECT scan (middle) shows reduced uptake in bilateral TPO regions. Delayed IMZ-SPECT scan (bottom) shows markedly reduced Bz receptor densities in bilateral TPO regions, but this decreased uptake is more extensive compared to that on the HMPAO and early IMZ-SPECT images.

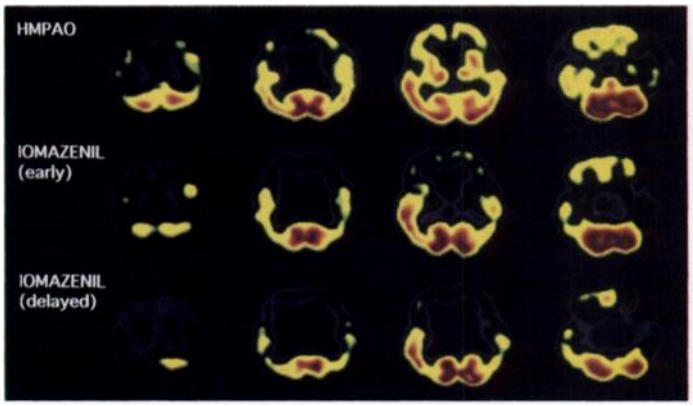


**FIGURE 2.** Patient 7, a 61-yr-old man with Alzheimer's dementia . HMPAO-SPECT (top) shows reduced uptake in bilateral frontal regions. Early IMZ-SPECT scan (middle) shows reduced uptake in the same regions as the HMPAO scan. Delayed IMZ-SPECT scan (bottom) shows markedly reduced Bz receptor densities in bilateral frontal regions. This decreased uptake is more extensive compared with that seen on the HMPAO and early IMZ-SPECT scans.

**TABLE 2**
SPECT Studies with Technetium-99m-HMPAO and Iodine-123-Iomazenil

| Patient no. | Decreased HMPAO uptake | Decreased uptake in IMZ-SPECT | | | HMPAO vs. IMZ | |
|---|---|---|---|---|---|---|
| | | Early (E) | Delayed (D) | E vs. D | Early | Delayed |
| 1 | bil. TPO (rt < lt) | bil. TPO | bil. TPO | E < D | CBF < BZ | CBF < BZ |
| 2 | bil. TPO | bil. TPO | bil. TPO | E < D | CBF < BZ | CBF < BZ |
| 3 | bil. TPO | bil. TPO | bil. TPO + parietal | E < D | CBF < BZ | CBF < BZ |
| 4 | bil. TPO (rt < lt) | bil. TPO (rt < lt) | bil. TPO (rt < lt) | E < D | CBF < BZ | CBF < BZ |
| 5 | bil. TPO + frontal | bil. TPO + frontal | bil. TPO + frontal | E < D | CBF < BZ | CBF < BZ |
| 6 | bil. frontal | bil. frontal | bil. frontal | E < D | CBF < BZ | CBF < BZ |
| 7 | bil. frontal | bil. frontal | bil. frontal + temporal | E < D | CBF < BZ | CBF < BZ |
| 8 | bil. frontal | bil. frontal | bil. frontal + parietal | E < D | CBF < BZ | CBF < BZ |

TPO = temporo-parieto-occipital; CBF = cerebral blood flow; bil. = bilateral; BZ = benzodiazepine receptor binding; E < D = Delayed IMZ-SPECT showing reduced uptake areas more extensively than early IMZ-SPECT; CBF < IMZ = IMZ-SPECT showing reduced uptake areas more extensively than HMPAO-SPECT; CBF < IMZ = IMZ-SPECT showing reduced uptake areas more extensively than or equal to HMPAO-SPECT.

depicted by IMZ-SPECT were more extensive than those of decreased cerebral blood flow (CBF).

### Iodine-123-IMZ Distribution

The results of quantitative analysis of IMZ distribution are shown in Table 3. The cerebrum-to-cerebellum ratio for the parietal lobe for the TPO hypoperfusion type of Alzheimer's disease group was significantly lower than that of the control group (0.84 versus 1.04, $p < 0.05$). The cerebrum-to-cerebellum ratio for the frontal lobe and the parietal lobe for the F hypoperfusion type of Alzheimer's disease group was significantly lower than that for the control group (0.86 versus 1.07, $p < 0.005$, 0.78 versus 1.04, $p < 0.01$).

## DISCUSSION

In this study, IMZ-SPECT was superior to HMPAO-SPECT in depicting the abnormal area in patients with probable Alzheimer's disease. These results indicate that Bz receptor imaging may be useful for detecting the disease in comparison to perfusion imaging.

We performed IMZ-SPECT acquisitions at two time points, 15 and 180 min after IMZ administration. The accumulation of IMZ in the brain varies minutely depending on tracer characteristics and regional tissue (*14*). Immediately after the injection, the distribution of IMZ results in images reflecting compound transport. Accordingly, early IMZ images are considered to be analogous to corresponding perfusion imaging with HMPAO. In this study, however, most of the early IMZ-SPECT images depicted different distribution patterns compared to the corresponding HMPAO-SPECT images. The discrepancy between early IMZ and HMPAO images may perhaps be explained as follows. Washout of the ligand from the free tissue pool that might start early in SPECT scanning and regional distribution of early IMZ-SPECT images was partially influenced. Another possibility is that IMZ is a better flow tracer than HMPAO because HMPAO is known to suffer from limited BBB extraction and trapping in cerebral gray matter (*15*). If early distribution of IMZ has a stronger relationship with rCBF than that of HMPAO, a small reduction of rCBF could be detected clearly in the early IMZ image. To solve this problem, comparison with $^{123}$I-N-isopropyl-p-iodoamphetamine (IMP) imaging is needed since IMP is almost completely extracted at a physiological flow rate (*16*). However, further studies are needed.

The delayed IMZ-SPECT images were also quite different from the rCBF images. The areas of decreased Bz receptor binding were more extensive than the areas of hypoperfusion in all patients. The present results suggest the possible uncoupling of blood flow and Bz receptor density in Alzheimer's disease. The degradation of inhibitory neuroreceptors, including Bz receptors, are not specific for the patients with Alzheimer's disease (*17*). Nevertheless, the reduction in the specific binding of IMZ in cortices most likely reflects neuronal damage because GABA/Bz chloride ionophore complex is widely distributed in the cerebral cortex (*18*). Thus, IMZ-SPECT may be a new approach for evaluating neuronal activity and detecting abnormalities in Alzheimer's disease. We did not perform the quantification of Bz receptor binding using compartmental analysis and other recently developed methods (*19,20*). However, Onishi et al. (*21*) reported that the images obtained 3 hr after bolus injection are very close to those of the distribution volume as well as the binding potential using table look-up procedures based on a three-compartment, two-parameter model. Accordingly, delayed IMZ images analyzed in this study may predominantly reflect specific binding.

Several studies of neuroreceptors using SPECT or PET imaging of ligands for Alzheimer's disease have been reported (*22,23*). In [$^{123}$I]-3-quinuclidinyl-4-iodobenzilate (QNB) studies of muscarinic acetylcholine receptor binding, which is one of the most affected neurotransmitters in Alzheimer's disease, focal cortical defects were shown in either the frontal or posterior temporal cortex in eight of 12 patients with Alzheimer's disease (*22*). Studies of $^{123}$I-QNB are currently limited because QNB is a nonspecific ligand which labels most or all of the muscarinic receptor sites and does not differentiate presynaptic from postsynaptic binding. Meyer et al. (*23*) reported PET studies using [$^{18}$F]-2-fluoro-2-deoxy-D-glucose (FDG) and

**TABLE 3**
Cerebrum-to-Cerebellum Activity Ratios for Various Cortical Areas in Control Subjects and Patients

| Area | Control | Alzheimer's disease | |
|---|---|---|---|
| | | Frontal type | TPO type |
| Frontal lobe | 1.07 ± 0.11 | 0.86 ± 0.05‡ | 1.04 ± 0.15 |
| Parietal lobe | 1.04 ± 0.15 | 0.78 ± 0.12† | 0.84 ± 0.19* |
| Temporal lobe | 1.18 ± 0.17 | 0.98 ± 0.15 | 1.01 ± 0.19 |
| Occipital lobe | 1.46 ± 0.15 | 1.20 ± 0.28 | 1.35 ± 0.21 |

*$p < 0.05$; †$p < 0.01$; ‡$p < 0.005$ against normal control value.
Data are expressed as mean ± s.d.

$^{11}$C-flumazenil (FMZ) and noted that the distribution volume (receptor binding) of FMZ was not affected in the parietal cortex where metabolic defect was detected with FDG in Alzheimer's subjects. The reason for the difference between the FMZ binding data and our data is unclear. The difference in binding characteristics between the two ligands, IMZ and FMZ must be considered. For example, IMZ has a tenfold higher affinity for its binding than FMZ at 37°C and the nonspecific uptake of FMZ is much higher than that for IMZ (*24*).

We could not include an adequate number of normal subjects, since all the patients were studied as a part of a Phase II or III clinical trial of IMZ in Japan (*25,26*). Therefore, to assess the diagnostic value of this new radiopharmaceutical, a greater number of normal individuals should be studied.

## CONCLUSION

IMZ-SPECT may be useful for the evaluation of the disease. The decline in Bz receptor density might provide a more accurate estimate of disease progression than reduction in rCBF.


## ACKNOWLEDGMENTS

The authors thank Nihon Medi-Physic Co., Ltd. for providing the [$^{123}$I] Iomazenil.


## REFERENCES


1. Holman BL, Johnson KA, Gerada B, Carvalho PA, Satlin A. The scintigraphic appearance of Alzheimer's disease: A prospective study using technetium-99m-HMPAO-SPECT. *J Nucl Med* 1992;33:181–185.
2. Cross AJ, Crow TJ, Ferrier IN, Johnson JA. The selectivity of the reduction of serotonin S2 receptors in Alzheimer-type dementia. *Neurobiol Aging* 1985;7:3–7.
3. Griffiths PD, Crossman AR. Receptor changes in the neocortex of postmortem tissue in Parkinson's disease and Alzheimer's disease. *Dementia* 1992;3:239–246.
4. Beer H, Bläuenstein PA, Hasler PH, et al. In vitro and in vivo evaluation of iodine-123-Ro 16–0154: A new imaging agent for SPECT investigations of benzodiazepine receptors. *J Nucl Med* 1990;31:1007–1014.
5. Cordes M, Henkes H, Ferstl F, et al. Evaluation of focal epilepsy: A SPECT scanning comparison of $^{123}$-I-iomazenil versus HMPAO. *AJNR* 1992;13:249–253.
6. Huffelen AC, Veelen JW. Identification of the side of epileptic focus with $^{123}$I-iomazenil SPECT. A comparison with $^{18}$F-FDG-PET and ictal EEG findings in patients with medically intractable complex partial seizures. *Acta Neurochir* 1990; 50(suppl):95–99.
7. Shimohama S, Taniguchi T, Fujiwara M, Kameyama M. Changes in benzodiazepine receptors in Alzheimer-type dementia. *Ann Neurol* 1988;23:404–406.
8. Mckhann G, Drachman D, Folsteinal M, Katzman R, Price P, Stadlar EM. Clinical diagnosis of Alzheimer's disease: Report of the NINCDS-ADRDA work group under the auspices of the department of health and human services task force on Alzheimer's disease. *Neurology* 1984;34:939–944.
9. Kimura K, Hashikawa K, Etani H, et al. A new apparatus for brain imaging: four-head rotating gamma camera single-photon emission computed tomography. *J Nucl Med* 1990;31:603–609.
10. Schubiger PA, Hasler PH, Beer-Wohlfahrt H, et al. Evaluation of a multicenter study with iomazenil—a benzodiazepine receptor ligand. *Eur J Nucl Med* 1991;12:569–582.
11. Yonekura Y, Nishizawa S, Tanaka F, et al. Phase 1 clinical study of $^{123}$I-iomazenil: a new probe to evaluate central-type benzodiazepine receptor with SPECT. *Jpn J Nucl Med* 1995;32:87–97.
12. Aquiloniws S, Eckerns A. *A color atlas of the human brain.* New York: Raven Press, 1980.
13. Onishi Y, Yonekura Y, Nishizawa, et al. Noninvasive quantification of iodine-123-iomazenil SPECT. *J Nucl Med* 1996;37:374–378.
14. Woods SW, Seibyl JP, Goddard AW, et al. Dynamic SPECT imaging after injection of the benzodiazepine receptor ligand [$^{123}$I] iomazenil in healthy human subjects. *Psych Res Neuroimag* 1992;45:67–77.
15. Lassen NA, Andersen AR, Friberg L, Paulson OB. The retention of [99mTc]-d,l-HM-PAO in the human brain after intracarotid bolus injection: a kinetic analysis. *J Cereb Blood Flow Metab* 1988;8:S13–S22.
16. Lear JL, Ackermann RF, Kameyama M, Kuhl DE. Evaluation of [$^{123}$I] isopropyliodo-amphetamine as a tracer for local cerebral blood flow using direct autoradiographic comparison. *J Cereb Blood Flow Metab* 1982;2:179–185.
17. Friedland RP, Brun A, Budinger TF. Pathological and positron emission tomographic correlation in Alzheimer's disease. *Lancet* 1985;1:228.
18. Hendry SHC, Schwark HD, Jones EG, Yan J. Numbers and proportions of GABA-immunoreactive neurons in different areas of monkey cerebral cortex. *J Neurosci* 1987;7:1503–1519.
19. Laruelle M, Baldwin RM, Rattner Z, et al. SPECT quantification of [123I] iomazenil binding to benzodiazepine receptors in nonhuman primates: I. kinetic modeling of single bolus experiments. *J Cereb Blood Flow Metab* 1994;14:439–452.
20. Abi-Dargham A, Laruelle M, Seibyl J, et al. SPECT measurement of benzodiazepine receptors in human brain with iodine-123-iomazenil: kinetic and equilibrium paradigms. *J Nucl Med* 1994;35:228–238.
21. Onishi Y, Yonekura Y, Mukai T, et al. Simple quantification of benzodiazepine receptor binding and ligand transport using iodine-123-iomazenil and two SPECT scans. *J Nucl Med* 1995;36:1201–1210.
22. Weinberger DR, Gibson R, Coppola R, et al. The distribution of cerebral muscarinic acetylcholine receptors in vivo in patients with dementia: a controlled study with $^{123}$IQNB and single-photon emission computed tomography. *Arch Neurol* 1991;48: 169–176.
23. Meyer MA, Koeppe RA, Frey KA, Foster NL, Kuhl DE. Positron emission tomography measures of benzodiazepine binding in Alzheimer's disease. *Arch Neurol* 1995;52:314–317.
24. Johnson EW, Woods SW, Zoghbi S, McBride BJ, Baldwin RM, Innis RB. Receptor binding characterization of the benzodiazepine radioligand $^{125}$I-Ro16–0154: potential probe for SPECT brain imaging. *Life Sci* 1990;47:1535–1546.
25. Torizuka K, Uemura K, Tohru M, et al. Phase 2 clinical study of $^{123}$I-iomazenil in various cerebral disease: part 2. Clinical evaluation of central-type benzodiazepine receptor imaging with $^{123}$I-iomazenil SPECT. *Jpn J Nucl Med* 1996;33:191–205.
26. Torizuka K, Uemura K, Tohru M, et al. Phase 3 clinical study of $^{123}$I-Iomazenil, a new central-type benzodiazepine receptor imaging agent (part 2): report on clinical usefulness in diagnosis of degenerative neurological diseases and mental disorders. *Jpn J Nucl Med* 1996;33:303–318.


# Brain Dopamine Transporter in Spontaneously Hypertensive Rats


Yoshiyuki Watanabe, Masahiro Fujita, Yasushi Ito, Tomoya Okada, Hideo Kusuoka and Tsunehiko Nishimura

*Division of Tracer Kinetics, Biomedical Research Center Osaka University Medical School, Osaka, Japan*



The brain dopamine system plays an important role in the development of hypertension. **Methods:** The amounts of the dopamine transporter (DAT) and dopamine D1 and D2 receptors in the brain were assessed by in vitro autoradiography with the ligands [$^{125}$I]β-CIT, [$^{125}$I]SCH23982 and [$^{125}$I]iodospiperone, respectively. Changes in this transporter and the two receptors were evaluated in spontaneously hypertensive (SH) rats and control (Wistar-Kyoto) rats at the prehypertensive (2-wk-old, n = 5) and posthypertensive (15-wk-old, n = 5) stages. **Results:** The β-CIT binding for the DAT was increased significantly in the caudate-putamen (CPu) of SH rats compared with that of Wistar-Kyoto (WKY) rats at both pre- and posthypertensive stages. In the evaluation of the lateral-to-medial CPu, the β-CIT binding on the lateral side was significantly higher than that on the medial side in SH rats at 2 wk. The SCH23982 binding for D1 receptor was increased significantly in CPu at posthypertensive SH rats. **Conclusion:** Increased DAT was found before the development of hypertension, and the increased DAT and D1 receptor were found at posthypertensive SH rats. The abnormal dopamine system contributes the development of hypertension, suggesting the possibility of diagnostic imaging for the essential hypertension.



**Key Words:** hypertension; iodine-125-β-CIT; dopamine transporter; dopamine receptor

**J Nucl Med 1997; 38:470–474**

Received Jan. 16, 1996; revision accepted Jun. 13, 1996.



For correspondence or reprints contact: Yoshiyuki Watanabe, MD, Division of Tracer Kinetics, Biomedical Research Center, Osaka University Medical School, 2-2 Yamadaoka Suita, Osaka 565, Japan.